Fall 10-4-2015

# Fracture behavior of high strength pearlitic steel wires

Bernhard Voelker
*Montanuniversität Leoben*, bernhard.voelker@unileoben.ac.at

Anton Hohenwarter
*Montanuniversität Leoben*

Reinhard Pippan
*Austrian Academy of Sciences*



## Recommended Citation

Y. Li, D. Raabe, M. Herbig, P.-P. Choi, S. Goto, A. Kostka, H. Yarita, C. Borchers and R. Kirchheim, Segregation Stabilizes Nanocrystalline Bulk Steel with Near Theoretical Strength, Phys. Rev. Lett. 113 (2014) 106104.

# FRACTURE BEHAVIOR OF HIGH STRENGTH PEARLITIC STEEL WIRES

B. Völker*[1], M. W. Kapp[2], R. Pippan[2] and A. Hohenwarter[1]

[1] Department Materials Physics, Montanuniversität Leoben, Jahnstrasse 12, 8700 Leoben, Austria
[2] Erich Schmid Institute of Materials Science of the Austrian Academy of Sciences, Jahnstrasse 12, 8700 Leoben, Austria

MONTAN UNIVERSITÄT WWW.UNILEOBEN.AC.AT

E S I

### *Motivation*

Pearlitic steel plays a very important role in industrial applications, for instance as railroad steel or in structural applications and thus, the interest to increase the strength of the material. One possibility to increase the strength of pearlitic steels is through deformation hardening. Earlier studies already investigated the increase in strength of pearlitic steels with increasing deformation and smaller cementite lamella spacing [1]. More recently, severe plastic deformation is used to increase the strength of pearlitic steels further, for instance high pressure torsion (HPT) deformation [2,3]. It has been shown that with increasing deformation the material increases its strength significantly. Utilizing wire drawing, even higher strengths were realized [4]. The wires presented here were drawn to strains up to 6.52 resulting in an ultimate tensile strength of 7 GPa which is the highest strength ever reached for a bulk material [2]. Additionally, Li et al. [2] revealed that after a certain strain the cementite lamellas dissolved in the ferrite matrix and a part of the graphite from the cementite decorates the grain boundaries.

In this investigation the directional dependence of the fracture toughness and the appearance of the corresponding fracture surfaces gives an insight in the dominating fracture mechanism.

## I. Experimental

### *Experimental setup and sample measurements*

Fracture mechanical experiments on pearlitic steel wires:

- Perpendicular to drawing direction (sample geometry *Figure 1*)
- In drawing direction (sample geometry *Figure 2*), prepared using FIB

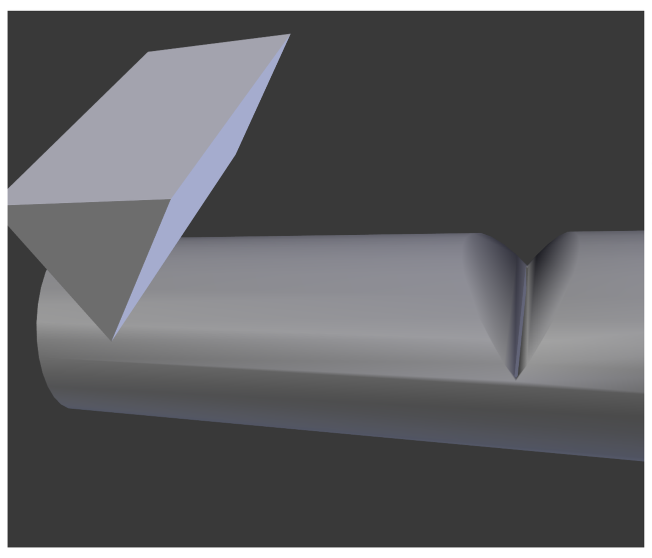

***Figure 1*** *Experimental setup for the fracture mechanic experiments of the perpendicular direction*

### *Sample measurements*

***Table 1*** *Measurements of the bending beams (perpendicular to drawing direction)*

| Wire | Number of Samples (-) | D (µm) | L (µm) |
|---|---|---|---|
| A | 1 | 120 | 800 |
| B | 1 | 24 | 140 |

***Table 2*** *Measurements of the in-situ micro-bending beams (drawing direction)*

| Wire | Sample | W (µm) | a (µm) | B (µm) | L (µm) |
|---|---|---|---|---|---|
| A | 1 | 7.3 | 1.4 | 6.2 | 28 |
| A | 2 | 7.2 | 1.3 | 5.6 | 28 |
| B | 1 | 1.8 | 0.7 | 1.5 | 7 |
| B | 2 | 2.5 | 0.8 | 2.4 | 10 |

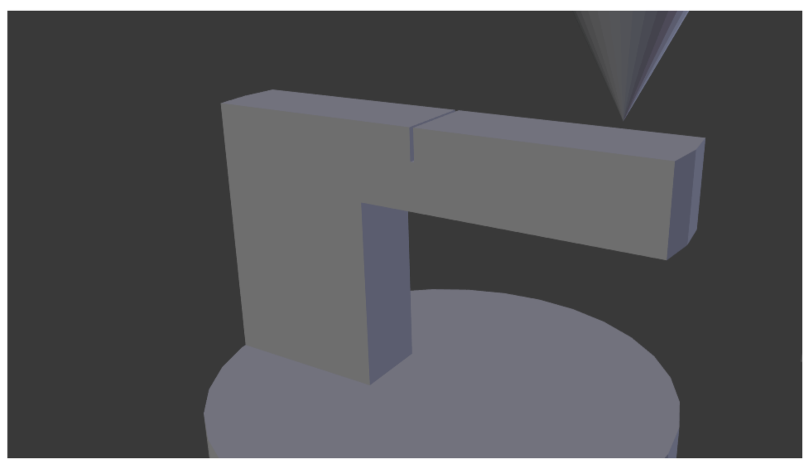

***Figure 2*** *Experimental setup for the fracture mechanical investigation of the pearlitic wire in drawing direction.*

## II. Results

### *Evaluation drawing direction*

$$K_Q = \frac{F_Q L}{B W^{\frac{3}{2}}} f\left({}^{a}/_{W}\right) \quad \text{Eq. 1}$$

$F_Q$ Fracture load
$f(a/W)$ Geometry factor according to *Eq. 2*
$K_Q$ Fracture toughness

$$f(a/W) = 4\,\frac{3(a/W)^{0.5}\left(1.23-(a/W)\left(1-(a/W)\right)\left(-6.09+13.96(a/W)-14.05(a/W)^2\right)\right)}{2\left(1+2(a/W)\right)\left(1-(a/W)\right)^{1.5}} \quad \text{Eq. 2}$$

$$CTOD_{calc} = d(n)\,\frac{K_Q^2}{E\sigma_y} \quad \text{Eq. 3} \qquad r_y = \frac{1}{2\pi}\left(\frac{K_Q}{\sigma_y}\right)^2 \quad \text{Eq. 4}$$

$d(n)$ Coefficient (0.5 for non-hardening materials)
$E$ Young's modulus (210 GPa)
$\sigma_y$ Yield strength (4 GPa - 100 µm wire and 7 GPa - 20 µm wire)
$CTOD_{calc}$ Calculated CTOD
$r_y$ Plastic zone size

***Table 3*** *Results of the in-situ micro-bending beams in drawing direction*

| Wire | Sample | $F_Q$ (mN) | f(a/W) (-) | $K_Q$ (MPam$^{1/2}$) | $CTOD_{calc}$ (nm) | $r_y$ (nm) |
|---|---|---|---|---|---|---|
| A | 1 | 4.6 | 4.81 | **5.1** | 15 | 255 |
| A | 2 | 4.1 | 4.61 | **4.9** | 14 | 238 |
| B | 1 | 0.23 | 8.34 | **3.7** | 4.7 | 45 |
| B | 2 | 0.51 | 7.00 | **3.8** | 4.8 | 46 |

### *Evaluation perpendicular direction*

$$K_Q = F_I \sigma_b \sqrt{\pi a} \quad \text{Eq. 5}$$

$F_I$ Stress intensity factor
$\sigma_b$ Bending stress at the surface
$K_Q$ Fracture toughness

***Table 4*** *Bending stress and fracture toughness of the samples perpendicular to the drawing direction. The significant difference in the $K_Q$ values arose due to the influence of the material bridges left on the edges of the pre-notch (see Figure 5b).*

| Wire | $K_Q$ (MPam$^{1/2}$) |
|---|---|
| A | 10.9 |
| B | 18.7 |

### *Fracture surfaces of samples in drawing direction*

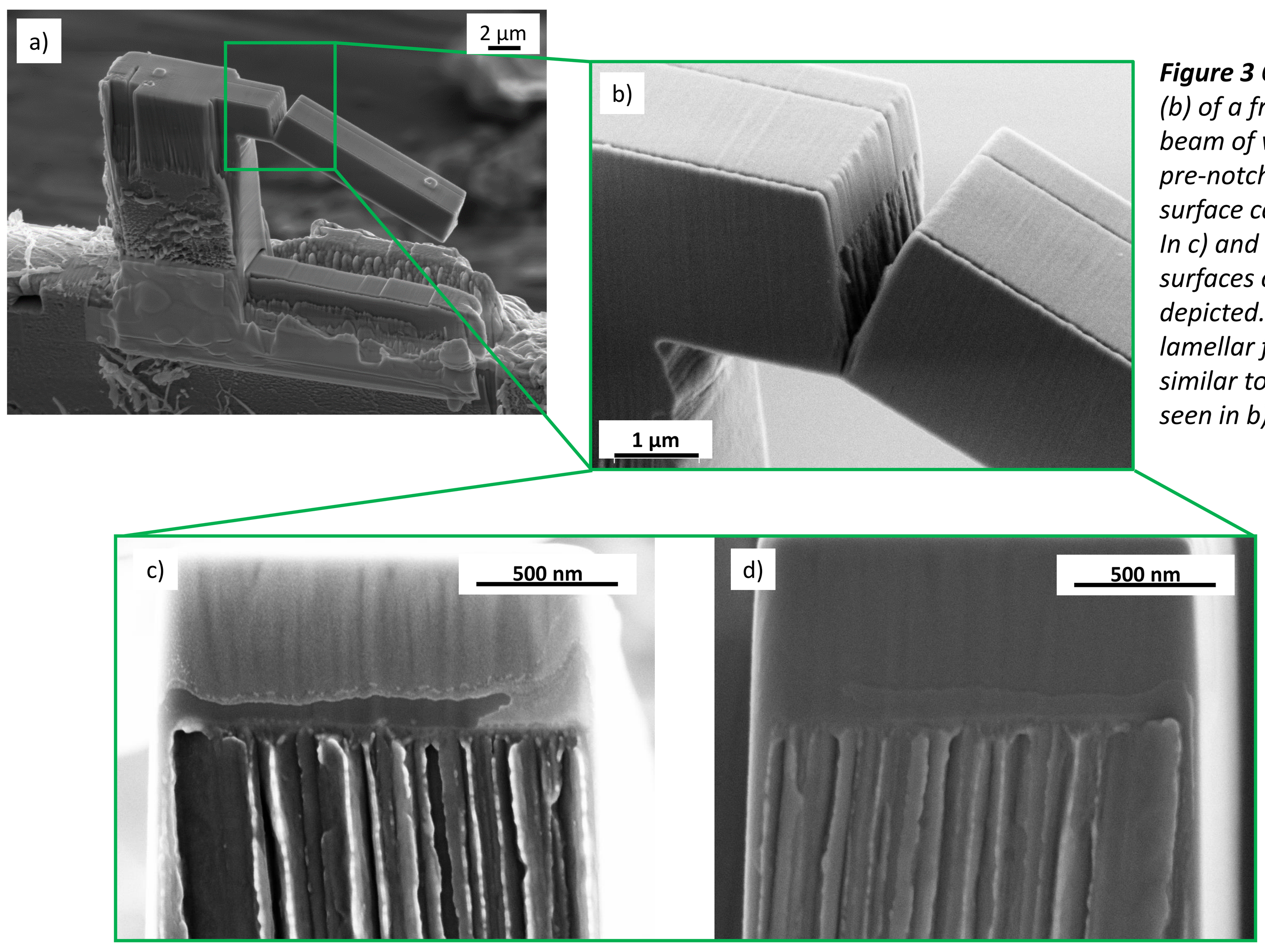


***Figure 3*** *Overview (a) and detail (b) of a fractured micro-bending beam of wire B (Sample 2). The pre-notch and the fracture surface can be distinguished. In c) and d) the two fracture surfaces of Sample 1 are depicted. The samples showed a lamellar fracture structure. This is similar to the fracture surface seen in b) for Sample 2.*

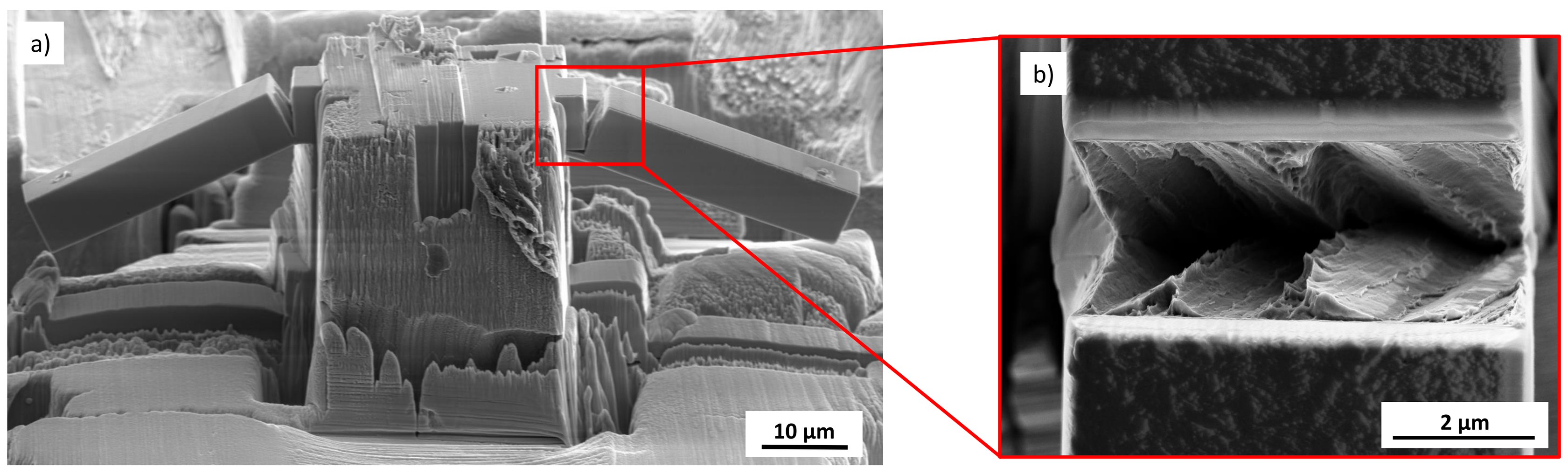


***Figure 4*** *In a) an overview image of the fractured micro-bending beams of wire A in drawing direction is depicted. A more detailed look at the fractured sample can be seen in image b). Here an lamellar appearance of the two fracture surfaces can be seen, which is similar to the fracture surfaces observed for wire B.*

### *Fracture surfaces of the samples in perpendicular direction*

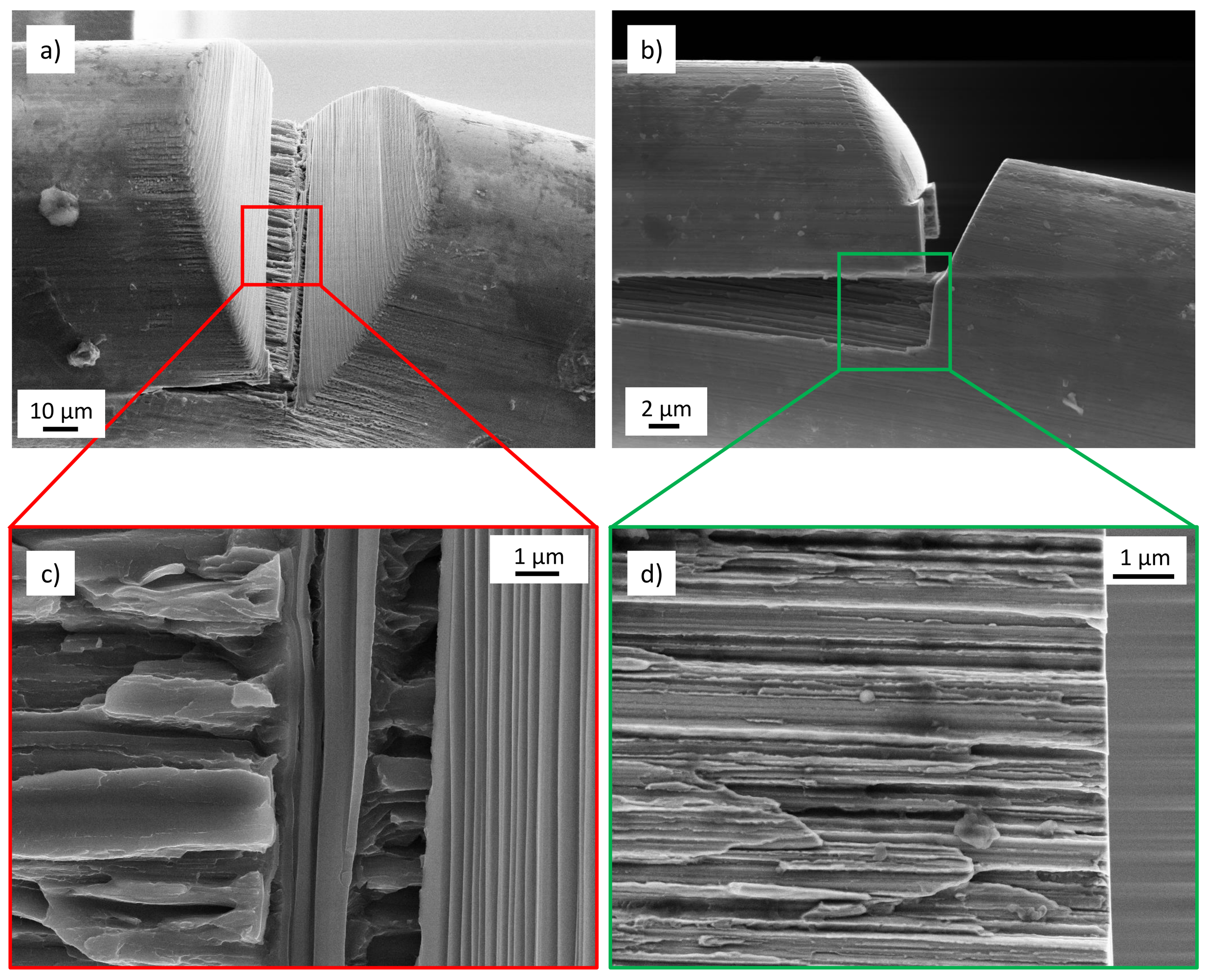


***Figure 5*** *Overview images of samples in the perpendicular testing direction. In a) the sample of wire A is shown and in b) wire B. In b) the thin material residue left on the edges of the notch is clearly visible. Additionally, both wires show a kinking of the crack which corresponds to a significantly lower fracture toughness along the drawing direction than in the perpendicular direction (at least half). In c) and d) detail images of the fracture surfaces. Both wires (A and B) show similar lamellar fracture surfaces as the micro-scale bending beams in drawing direction.*

### *Load-displacement curves*

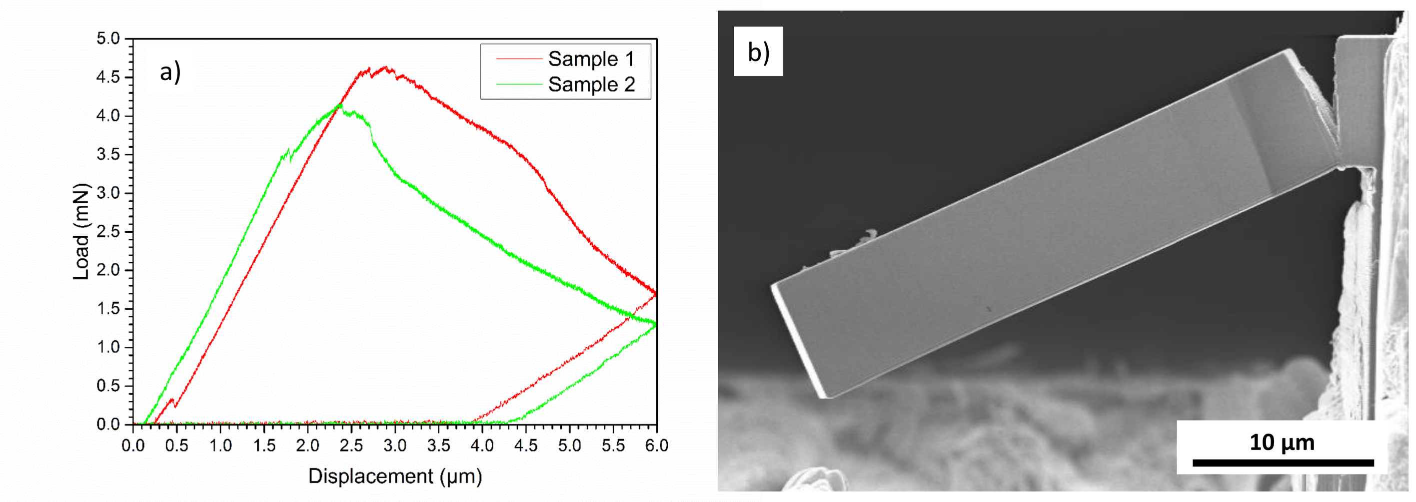


***Figure 6*** *a) Load-Displacement curves of wire A in drawing direction. Both Samples were tested utilizing an ASMEC, UNAT micro-indenter. b) Overview of a tested sample.*

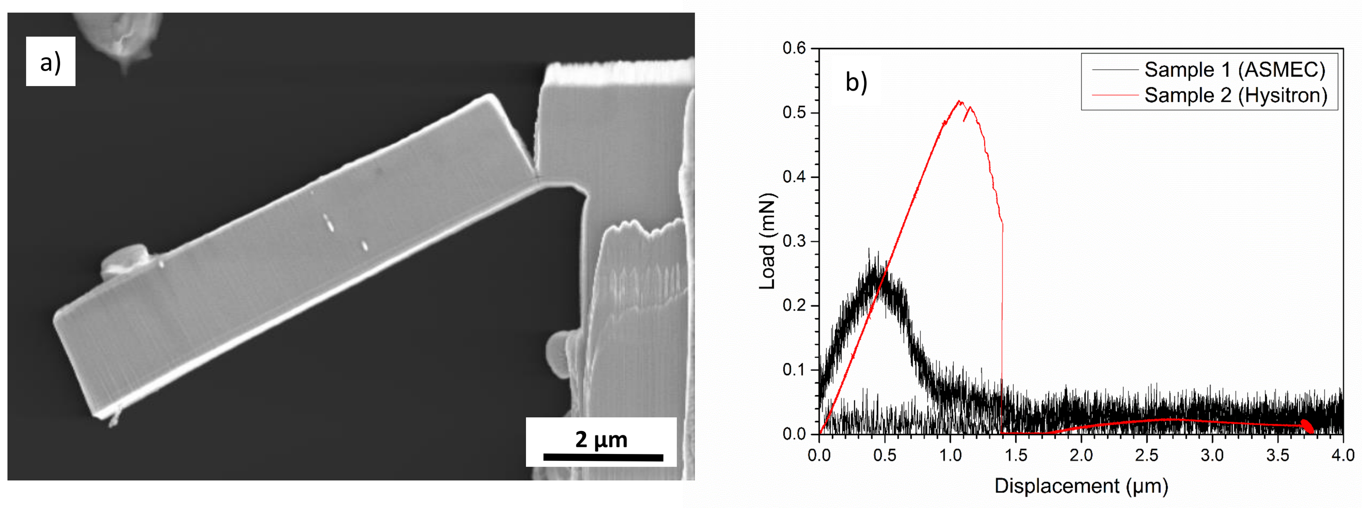


***Figure 7*** *Overview of a fractured micro-bending beam (a) of wire B (Sample 1) and the corresponding load-displacement curves (b). The load-displacement curve in b) are recorded using a ASMEC, UNAT micro-indenter (Sample 1) and a Hysitron Pico-Indenter, PI-85 (Sample 2).*

## III. Conclusion

- The investigated pearlitic steel wires show a very low fracture toughness in drawing direction. The value is comparable to the one of pearlitic steel deformed via high pressure torsion material [3].
- Due to the low fracture toughness in drawing direction there is not much plastic deformation present in the samples. This is also seen in the estimated plastic zone size which is relatively small compared to the micro-bending beam measurements (less than 5%).
- The fracture surfaces for wires A and B show a similar appearance. In contrast to that, a different fracture structure would be expected according to Li et al. [4], who reported that for wire A, with a drawing strain of 3.1, there are still cementite lamellas present, but for wire B, with a drawing strain of about 6.7, the cementite lamellas are dissolved.
- The fracture toughness perpendicular to the drawing direction is significantly larger than the one in drawing direction. The calculated values for the perpendicular direction represent a lower boundary due to the crack deflection.
- The difference in fracture toughness of the perpendicular direction is due to the thin material bridges left at the edges of the FIB pre-notch.

## Acknowledgements

This Project is funded by the Austrian Science Fund (FWF) under Project number P26729-N19. The Authors would like to thank Yujiao Li and Dierk Raabe of the "Max-Planck-Institut für Eisenforschung" for providing the pearlitic steel wires.

## References

[1] J.D. Embury, R.M. Fisher, The structure and properties of drawn pearlite, Acta Metallurgica. 14 (1966) 147–159.
[2] Y. Ivanisenko, W. Lojkowski, R.Z. Valiev, H.-J. Fecht, The mechanism of formation of nanostructure and dissolution of cementite in a pearlitic steel during high pressure torsion, Acta Materialia. 51 (2003) 5555–5570.
[3] A. Hohenwarter, A. Taylor, R. Stock, R. Pippan, Effect of Large Shear Deformations on the Fracture Behavior of a Fully Pearlitic Steel, Metall and Mat Trans A. 42 (2010) 1609–1618.
[4] Y. Li, D. Raabe, M. Herbig, P.-P. Choi, S. Goto, A. Kostka, H. Yarita, C. Borchers, R. Kirchheim, Segregation Stabilizes Nanocrystalline Bulk Steel with Near Theoretical Strength, Phys. Rev. Lett. 113 (2014) 106104.

*Corresponding author: bernhard.voelker@unileoben.ac.at